Proceedings of the 1995 IEEE International Symposium on EMC, Atlanta, August 1995, pp. 490-495

Definition, Relevance and Measurement of the Parallel and Axial Transfer Impedances

F. Broydé, E. Clavelier
EXCEM
12, Chemin des Hauts de Clairefontaine
78580 MAULE - FRANCE
tel: (1) 34 75 13 65 fax : (1) 34 75 13 66

Abstract— The present paper is focused on the definition, evaluation and measurement of two of the five possible types of coupling on multiconductor cables, which have recently been identified in the litterature : the parallel transfer impedance and the axial transfer impedance coupling. The definitions of these two parameters are presented and discussed. We then give two complete examples of field-to-cable coupling calculations, with these types of coupling included. An experiment reproducing the set-up considered in our calculations shows the relevance of parallel and axial transfer impedances. Two new devices for the measurements of these quantities are then presented, and measurement results are given for several single-shield multiconductor cables.

I. Introduction

Recent papers [3], [7], [8], [9] outlined that coupling mechanisms other than those characterized by the per-unit-length transfer impedance (type 1 coupling) and the radial electric coupling coefficient [4] (type 2 coupling), may exist on multiconductor shielded cables, and gave a mostly theoretical introduction to three new types of coupling, called type 3, type 4 and type 5 couplings. A conventional treatment of type 1 and type 2 couplings on multiconductor cables appear in [1] and [2] § 6.5. The new types of coupling are :

— type 3 coupling, which is related to the incident magnetic field, and for which the cable is characterized by an axial transfer impedance (in Ω) ;

— type 4 coupling, which is related to the incident electric field, and for which the cable is characterized by a dimensionless parallel electric coupling coefficient ;

— type 5 coupling, which is related to the magnetic incident field, and for which the cable is characterized by a parallel transfer impedance (in Ω) ;

The present paper will be focused on type 3 (or axial tranfer impedance coupling) and type 5 (or parallel transfer impedance coupling) only. It first recalls the definitions of the five main types of coupling (§ II). It will then describe a canonical experiment where each of the different coupling types contributes to a portion of the voltage measured at one end of the multiconductor cable (§ III). We will then show on § IV how this experiment was conducted in GTEM cell, and show a sample of our results, that can only be explained with the introduction of mechanisms other than type 1 and type 2 couplings.

We will then present two measurement methods (in § V and § VI) that apply the magnetic field locally to the cable, and characterize the cable at this point. The first method [5], [7], [8] involves a "parallel H-field probe". The second method [6], [9] is based on an "axial H-field probe".

II. Definitions of the Five Main Types of Coupling

Let us consider a multiconductor shielded cable, which may contain an arbitrary positive integer number, n, of internal wires (which may include internal cable shields), with the two following assumptions :

— the shield has a perfect cylindrical symmetry.
— the shield is effective : by this we mean that it offers enough screening for the weak coupling approximation to be valid.

Under the weak coupling approximation, a stimulus on one side (side 1) of the shield may effect the current and charges on the other side (side 2) of the screen or shield, but these effects have negligible consequences on charges and current on the side (side 1) where the stimulus is applied. Therefore, even though the cable as a whole does not have the cylindrical symmetry, in the case of an external excitation, the current on the screen establishs itself as if the cylindrical symmetry was present.

With these two hypothesis, at least five different types of coupling can occur (this number of types is not limited to five, as explained in the last remark of [3] § III and in the conclusion of [8]). These types of couplings will be explained with figures which represent a shielded pair, having three obvious planes of symmetry. This representation was used for clarity in our drawings, but the cable may have any number of internal wires, and no symmetry need be assumed, though it may actually be present.

Fig. 1 illustrates type 1 coupling. The characteristics of the cable for this coupling may be expressed with n linear transfer impedances (one for each internal wire), as mentioned in the introduction. On an elementary length dx of cable, type 1 coupling causes a voltage dv_α to be induced on the αth internal conductor, equal to :

$$dv_\alpha = Z_{T\alpha}\, i_{MC}\, dx \qquad (1)$$

where $Z_{T\alpha}$ is the linear transfer impedance of the cable with respect to the wire α, and i_{MC} is the current on the cable screen. Note that "linear transfer impedance" is used as synonimous with "per-unit-length transfer impedance".

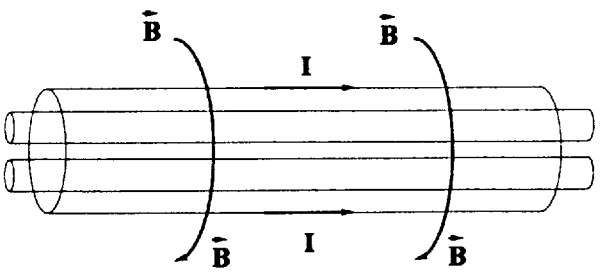

Fig. 1. Type 1 coupling on a shielded multiconductor cable.

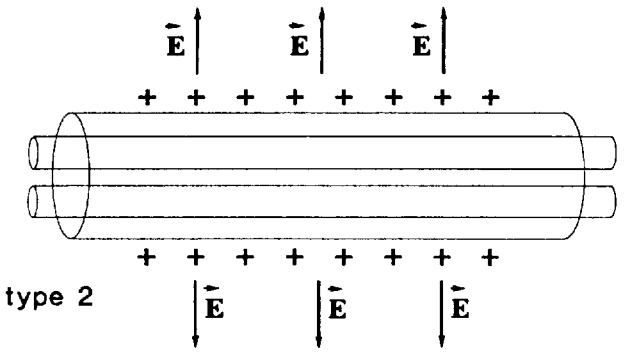

Fig. 2. Type 2 coupling on a shielded multiconductor cable.

Fig. 2 illustrates type 2 coupling. The cable could be characterized for this type of coupling with n radial electric coupling coefficients, which are a property of the cable (shield and internal wires) alone. Type 2 coupling produces a current di_α on the αth internal conductor when a charge dq_0 accumulates on the cable screen, on an elementary length dx of cable. This current is equal to :

$$di_\alpha = j\omega \zeta_{R\alpha}\, dq_0 \tag{2}$$

where $\zeta_{R\alpha}$ is the radial electric coupling coefficient for the wire α.

Fig. 3 illustrates type 3 coupling. Here the current is circumferencial, and the magnetic field is axial. This is typically what would be observed if the cable is placed on the axis of a solenoïd. Coupling to the internal wires will not occur if these wires are straight. However, a voltage will clearly be induced on skewed wires, an example of which is the twisted pair. It does not seem appropriate to relate the induced voltage to the current in the coil. We prefer to introduce a quantity that relates the voltage per unit length on a given wire to the axial magnetic field **H** (in A/m). We shall call this quantity the axial transfer impedance (in Ω), and we need n axial transfer impedances to characterize the cable with respect to type 3 coupling. Type 3 coupling produces a voltage dv_α on the internal conductor α, for an elementary length dx of cable. This voltage is equal to :

$$dv_\alpha = Z_{AT\alpha}\, H_\varphi\, dx \tag{3}$$

where $Z_{AT\alpha}$ is the axial transfer impedance for the internal wire α, and H_φ is the field strength of the axial magnetic field.

Fig. 4 illustrates type 4 coupling. An electric field perpendicular to the cable axis is present. Its orientation around the cable is such that it produces no net charge per unit length of cable. This is what would happen if the cable is introduced at the center of two parallel plates excited by a symmetrical voltage source. This coupling can be described by a quantity that relates the per-unit-length current received on a wire to the per-unit-length displacement current that flows into the cable on one side and leaves it on the other. We call this quantity the parallel electric coupling coefficient. As usual we need n such complex quantities to characterize the cable with respect to type 4 coupling, but it must be emphasized that these are *a priori* dependant on the orientation of the electric field. The incident field produces zero charge on any length of cable, because of the cancellation of two opposite charges on the top and bottom of the screen. If dq_1 is one of the two charges, the electric field will produce a current di_α on the αth conductor for an elementary length dx of cable. This current is equal to :

$$di_\alpha = j\omega \zeta_{P\alpha}\, dq_1 \tag{4}$$

where $\zeta_{P\alpha}$ is the parallel electric coupling coefficient for the wire α, in the direction of the incident field.

Fig. 5 illustrates type 5 coupling. A magnetic field passes through the cable, penetrates the shield and directly induces voltages between the cable's internal conductors. This type of coupling would be produced if the cable is installed inside an Helmholtz coil, orthogonal or perpendicular to the axis of the magnetic field. We propose to describe this phenomenon with a quantity defined for each inner wire as the ratio between the per-unit-length voltage induced with respect to cable shield, to the amplitude of the impinging magnetic field (in A/m). We call this quantity the parallel transfer impedance of the cable (in Ω). As previously, we need n complex parallel tranfer impedances, which are *a priori* dependant on the orientation of the magnetic field. Type 5 coupling produces a voltage dv_α on the αth internal conductor, for an elementary length dx of cable. This voltage is equal to :

$$dv_\alpha = Z_{PT\alpha}\, H_\perp\, dx \tag{5}$$

where $H_\perp$ is the field strength of the orthogonal magnetic field and $Z_{PT\alpha}$ is the parallel transfer impedance for the wire α, in the direction of the incident magnetic field.

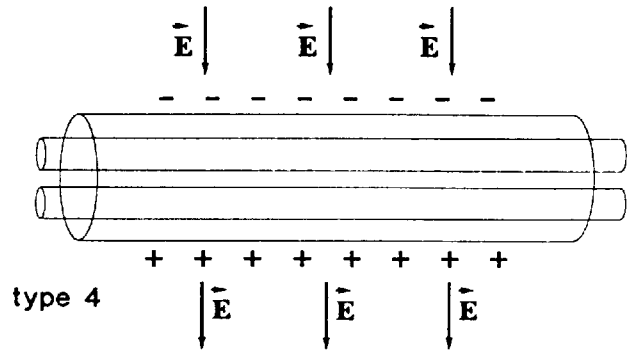

Fig. 4. Type 4 coupling on a shielded multiconductor cable

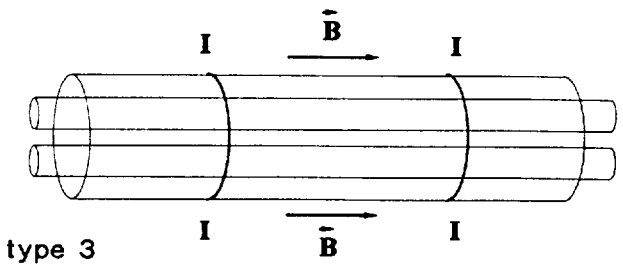

Fig. 3. Type 3 coupling on a shielded multiconductor cable.

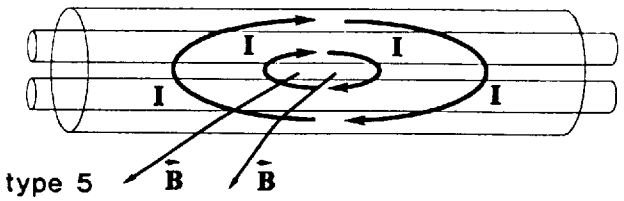

Fig. 5. Type 5 coupling on a shielded multiconductor cable.

From the above definitions it is clear that for a coaxial cable with perfect symmetry, the axial transfer impedance, the parallel electric coupling coefficient and the parallel transfer impedance all vanish. This would not necessarily be true for an imperfect coaxial cable.

The above definitions can easily be extended to cables of circular or almost circular cross-section, without assuming perfect cylindrical symmetry. Obviously, for such a cable, the idea of defining five coupling modes can be kept, provided they are defined according to the symmetry of the incident field, as it appears in the definition given previously (a discussion of this point is presented in [1]).

III. Calculation of Field-To-Cable Coupling

In this section the complete expression for the voltage on any internal wire is given for two examples of field-to-cable coupling problems, namely when the wave vector of the incident wave is longitudinal (i.e. parallel) and transverse (i.e. broadside) to a short cable laying on a ground plane. Our calculation is valid for any cable of circular or almost circular cross-section, but assumes a length of cable electrically short, because we did not consider internal reflections or long line effects. We have also neglected crosstalk between internal wires, the influence of which would be negligible under our assumptions : for a short length of cable, the field-to-internal wire coupling is a first order phenomenon, while amplitudes resulting from capacitive and inductive coupling between internal wires are second order quantities, because they are the result of both field-to-internal wire coupling and crosstalk coupling, therefore involving the product of *two* unwanted (hence presumably small) coupling mechanisms. The relative magnitude of these first and second order effects could be discussed for specific values of the **C** matrix and **L** matrix of the internal wires, and terminating impedances, but this is not within our present scope.

The computation technique was presented in [3] and will not be repeated here. It involves, in the case of the longitudinal incidence, the calculation of the charge and current densities on the cable laying on the ground plane. Our results assume that the current distribution is the "high frequency" distribution, characterized by strong skin and proximity effects, the surface current density differing from the charge distribution by a multiplying coefficient. This assumption is typically valid above 100 kHz for cables of interest.

In the case of the longitudinal incidence, a wave propagates along a cable in galvanic contact with the metallic ground plane. This situation is typically what would be obtained if a cable is installed transversly on the floor of a rectangular TEM cell or a GTEM cell, as shown on fig. 6. On the internal wire α, terminated at its port 1 by a linear load of impedance $Z_{1\alpha}$ connected to ground, and at its port 2 by a linear load of impedance $Z_{2\alpha}$ connected to ground , we find the disturbance voltages :

where $v_{1\alpha}$ and $v_{2\alpha}$ are respectively the voltages at port 1 and 2 ;
l is the length of cable exposed to the incident field ;
$\langle Z_{PT\alpha} \rangle$ is the averaged $Z_{PT\alpha}$ in the direction of the magnetic field ;
$\langle \zeta_{P\alpha} \rangle$ is the averaged $\zeta_{R\alpha}$ in the direction of the electric field ;
r_0 is the radius of the cable (assumed of circular cross-section) ;
E_0 and H_0 are the applied fields, assumed homogeneous and oriented as if the wave was plane along the cable length.

The above results neglect the αth wire impedance and admittance to ground, and are therefore not valid if the impedance of the terminations connected in series, is not large compared to the wire impedances, or if the admittance of the terminations connected in parallel, is not large compared to the wire admittance with respect to ground.

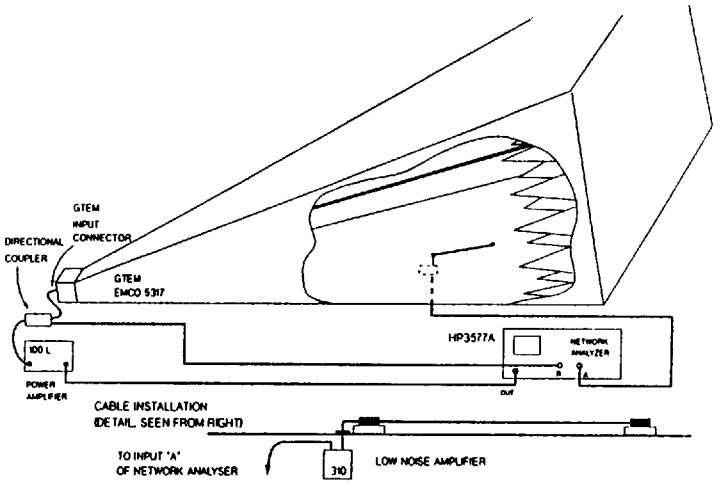

Fig. 6. The longitudinal installation of a cable under test inside a GTEM cell.

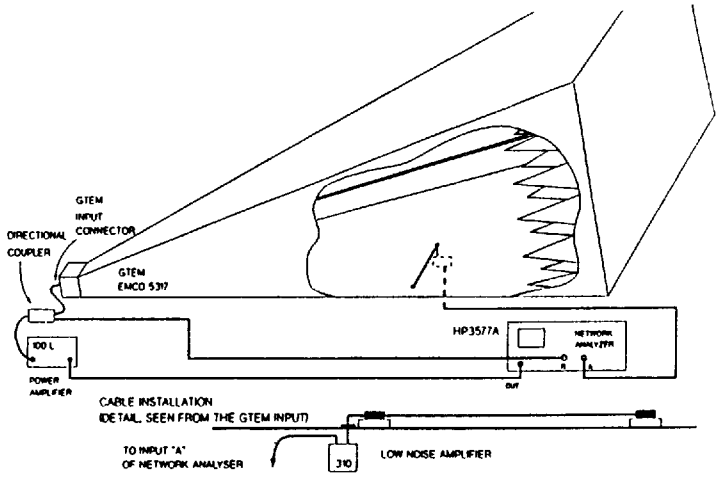

Fig. 7. The transverse installation of a cable under test inside a GTEM cell.

$$v_{1\alpha} = \frac{\ell H_0 Z_{1\alpha}}{\left(Z_{1\alpha} + Z_{2\alpha}\right)} \left\{ \left\langle Z_{PT\alpha} \right\rangle + 2\pi r_0 Z_{T\alpha} \right\} + \frac{j\omega \varepsilon_0 \ell E_0 Z_{1\alpha} Z_{2\alpha}}{\left(Z_{1\alpha} + Z_{2\alpha}\right)} r_0 \left\{ \left\langle \zeta_{P\alpha} \right\rangle - \pi \zeta_{R\alpha} \right\} \qquad (6)$$

and

$$v_{2\alpha} = \frac{-\ell H_0 Z_{2\alpha}}{\left(Z_{1\alpha} + Z_{2\alpha}\right)} \left\{ \left\langle Z_{PT\alpha} \right\rangle + 2\pi r_0 Z_{T\alpha} \right\} + \frac{j\omega \varepsilon_0 \ell E_0 Z_{1\alpha} Z_{2\alpha}}{\left(Z_{1\alpha} + Z_{2\alpha}\right)} r_0 \left\{ \left\langle \zeta_{P\alpha} \right\rangle - \pi \zeta_{R\alpha} \right\} \qquad (7)$$

Let us now consider the case of a cable the shield of which is in contact with a metallic plane, but installed so that the cable is transverse to the direction of propagation of a wave propagating in a direction parallel to the plane, the other previous hypothesis remaining. Once again, this situation may be obtained in a rectangular TEM cell or a GTEM cell, as shown on fig. 7 (in the case of the GTEM cell, the cable should be bended because the incident wave is supposed to be spherical). On the wire α, terminated as above, we now find the voltages :

$$v_{1\alpha} = \frac{\ell H_0 Z_{1\alpha}}{\left(Z_{1\alpha}+Z_{2\alpha}\right)} Z_{AT\alpha} + \frac{j\omega\varepsilon_0 \ell E_0 Z_{1\alpha} Z_{2\alpha}}{\left(Z_{1\alpha}+Z_{2\alpha}\right)} r_0 \left\{ \left\langle \zeta_{P\alpha} \right\rangle - \pi \zeta_{R\alpha} \right\} \tag{8}$$

and

$$v_{2\alpha} = \frac{-\ell H_0 Z_{2\alpha}}{\left(Z_{1\alpha}+Z_{2\alpha}\right)} Z_{AT\alpha} + \frac{j\omega\varepsilon_0 \ell E_0 Z_{1\alpha} Z_{2\alpha}}{\left(Z_{1\alpha}+Z_{2\alpha}\right)} r_0 \left\{ \left\langle \zeta_{P\alpha} \right\rangle - \pi \zeta_{R\alpha} \right\} \tag{9}$$

These last expressions are of great interest because the type 3 coupling coefficient, $Z_{AT\,\alpha}$, is the only term that is independant of the electric field on the cable : if an electric screen is installed above the cable, reducing the electric field but not the magnetic field around the cable, this term shall not be reduced.

Measurements on a coaxial cable installed in a TEM or GTEM cell for the transverse incidence can therefore lead to the determination of the axial transfer impedance of a cable. Formulas (6) to (9) contain improvements and corrections to previously published results [3], [7], [8] and [9]. Notice that averaged quantities have been used when the cable parameter is dependant on the θ angle of cylindrical coordinates.

IV. Measurement Results in a GTEM Cell

The measurements defined in the last section have been performed in a GTEM Cell with the following larger dimensions : 7.7 m by 4.1 m by 3.1 m (model EMCO 5317). These measurements are an improved version of a work already published [1], conducted at only 2 frequencies in a conventional TEM cell. The experimental set-up is described on fig. 6 and fig. 7, and all measurements were done after a calibration of the internal field at the spot where the cable sample was installed. We will show some results obtained for our sample C10, configuration B : this is a single shield cable with a screen diameter of about 4.2 mm, with six internal wires. The sample is 55 cm long fitted with special connectors, configuration B refering to a measurement made on a conductor grounded at the opposite connector. It may reasonably be accepted that such a sample can be regarded as electrically short up to 10 MHz at least.

Fig. 8 shows our results for the longitudinal installation, and fig. 9 the results for the transverse installation. They are expressed as effective heights in dB(m), because the voltage measured (with a 50 Ω instrument) at one end of the sample, is normalized to 1 V/m of applied field. We made sure that the cable response was not related to an electric field coupling mechanism (type 2 or type 4 coupling). As from 2.8 MHz, it is very interesting to notice that the cable response is larger in the transverse orientation as it is in the longitudinal one. It is not possible to understand this result if one thinks only in term of type 1 coupling !

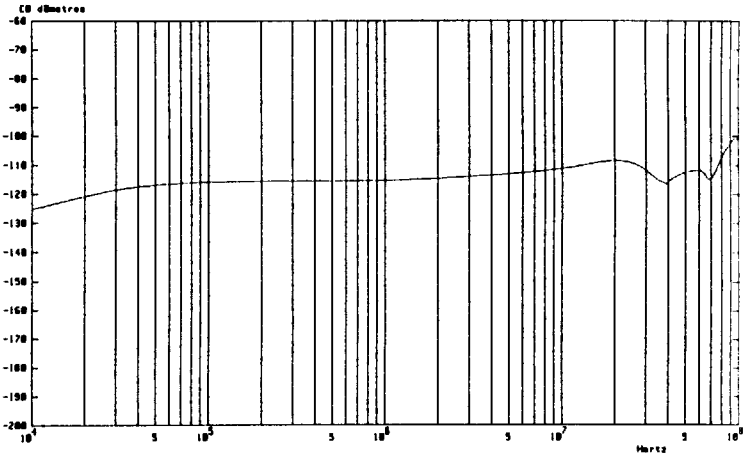

Fig. 8. Effective height in dB(m) measured for the longitudinal installation.

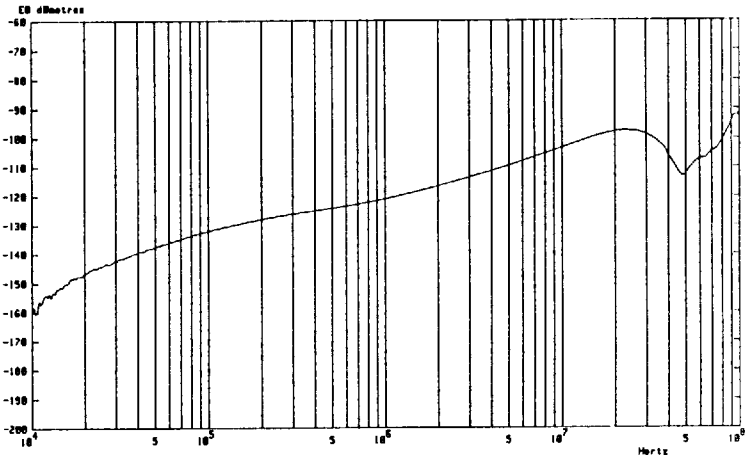

Fig. 9. Effective height in dB(m) measured for the transverse installation.

V. Measurements with a Parallel H-Field Probe

Fig. 10 shows a parallel H-field probe [5]. This new device includes a plastic material structure (2) designed to allow the introduction of a cable under test (6), an N-type input receptacle (3), a slotted ferrite toroidal core (4) and a coil (5) wound around the core. When driven by a sinusoidal generator, this device produces a "parallel" magnetic field transverse to the cable axis, and is therefore suitable for the measurement of the parallel transfer impedance Z_{PT}. Because it is not possible to create an homogeneous field on a given portion of the cable, and a zero field elsewhere, the parallel H-field probe requires a calibration, which can be achieved by using it to measure the parallel transfer impedance of a standard cable, such as one made of two accurately manufactured parallel conductors.

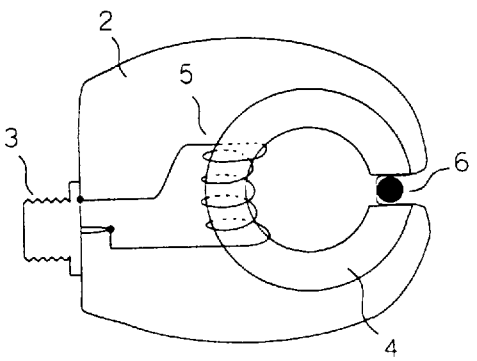

Fig. 10. A parallel H-field probe.

After preliminary measurements with our ZPT1/pr1 prototype parallel H-field probe [7] [8], more thorough measurements have been carried out with a new ZPT1/pr2 probe [9]. The useful bandwidth of this instrument exceeds 30 MHz. Active H-field probes are under development, and should improve this bandwidth to over 100 MHz, with an increased field strength. The parallel tranfert impedance of our cable sample C10, configuration B, is shown on fig. 11 : curve "a" is the one that is obtained for the orientation of the parallel field that produces the maximum response, while curve "b" is obtained for the orientation that produces the minimum response. Below 70 kHz, the parallel transfer impedance was too small to be measured with our simple set-up, and noise dominates, whereas above 30 MHz, the behaviour of the H-field probe itself becomes questionable, because it is not matched to the generator, and this mismatch is only partially corrected for by the calibration.

The cable sample C10 was also used in configuration A : in that case the instrument for voltage measurement is connected, at the connector A, to an internal wire which, at the opposite end (connector B) is only connected to an other internal wire, this last wire being grounded in the connector A. In that case, the quantity being measured is the difference of two parallel transfer impedances, that is to say, a differential mode parallel transfer impedance. The measured differential mode parallel transfer impedance is presented on fig. 12, the meaning of the curves "a" and "b" being the same as on fig. 11.

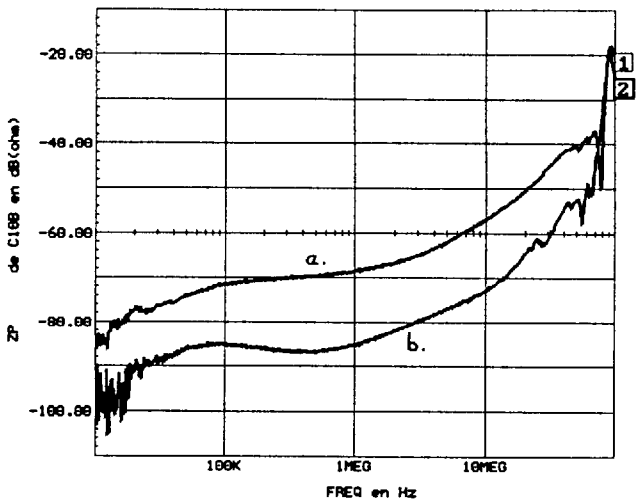

Fig. 11. Parallel transfer impedance of a wire of cable C10.

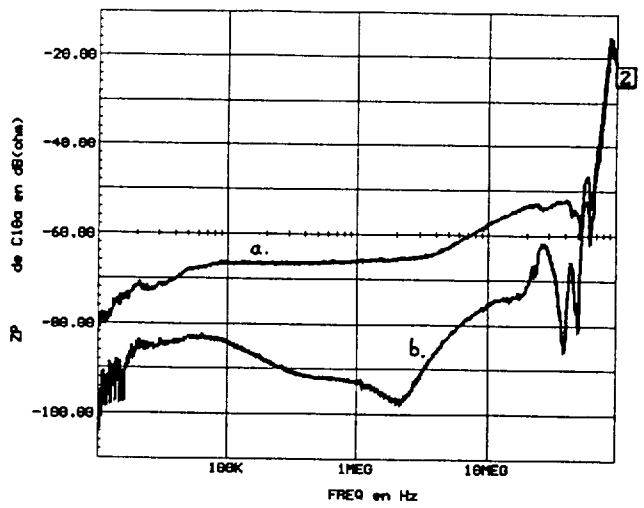

Fig. 12. Differential mode parallel transfer impedance of two wires of cable C10.

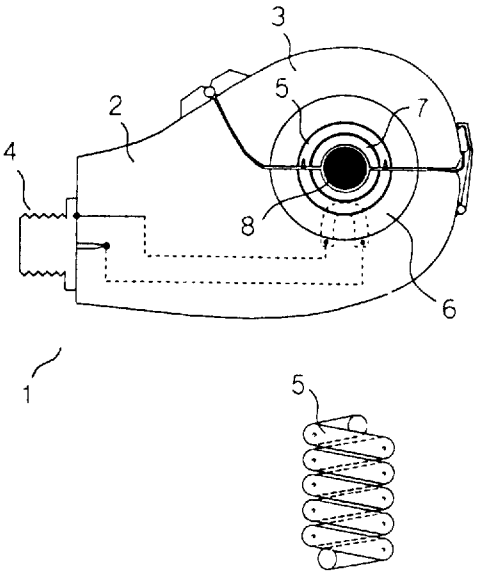

Fig. 13. An axial H-field probe

VI. Measurements with an Axial H-Field Probe

Fig. 13 shows an axial H-field probe [6]. This new device includes two plastic material structures (2), (3) forming a clamp, and designed to allow the introduction of a cable under test (8) having its axis perpendicular to the drawing. The parallel H-field probe has an N-type input receptacle (4), a slotted ferrite cylindrical core (6) split into two halves, and a coil (5) wound in the middle of the core, its axis perpendicular to the drawing. A cylindrical spacer (7) allows an appropriate centering of the cable (8), near the axis of the coil. When driven by a sinusoidal generator, this device produces an "axial" magnetic field on the cable, and is therefore suitable for the measurement of the axial transfer impedance Z_{AT}. Because it is not possible to create a homogeneous field on a given portion of the cable, and a zero field elsewhere, the axial H-field probe requires a calibration, which may be achieved with a standard cable, for instance made of an accurately manufactured helicoïdal conductor and a straight return conductor on the axis of this helix.

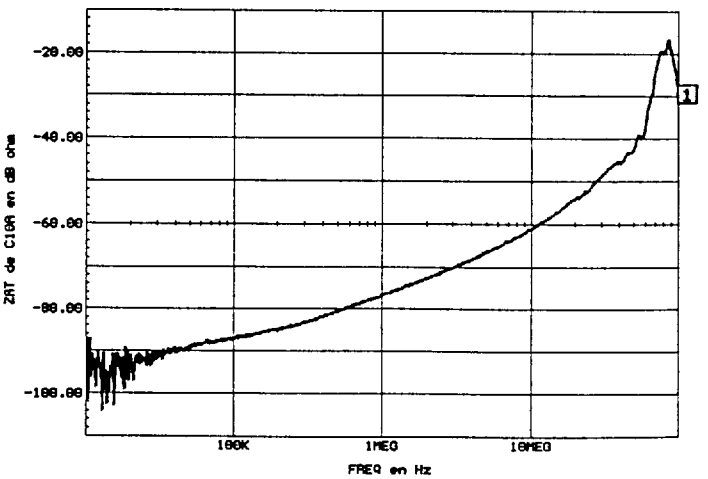

Fig. 14. Differential mode axial transfer impedance of two wires of cable C10.

Fig. 14 shows a measurement of axial transfert impedance, on the cable C10 in configuration A, with our axial H-field probe ZAT1/pr1. This results is in fact a difference of the axial transfer impedances of two wires, namely a differential mode axial transfer impedance.

VII. Conclusion

Five different types of coupling mechanisms have been explained for multiconductor shielded cables of circular or almost circular cross-section. We gave experimental evidence of the existence of coupling type 3 and coupling type 5, by performing global measurements in a GTEM cell, and local measurements with a parallel H-field probe and an axial H-field probe.

As was pointed out in [3] and [8], there is, from a theoretical point of view, a need for more than five types of coupling, if one intends to fully characterize an arbitrary multiconductor cable of almost circular cross-section. However, because actual cables are not *that* arbitrary, we *believe* that the five types of coupling presented here are suitable for an accurate enough description of the cable behaviour. This is why we now refer to these five types of coupling as the five *main* types of coupling.

Discussions with many colleagues concerning our "five main types of coupling theory" lead us to insist on the following :

1. The theory that describes the five main types of coupling takes into account a more complete development of the fields surrounding the cables than an approach limited to type 1 and type 2 couplings. However, the need for such a development has nothing to do with the presence of higher order modes of propagation for the external problem (modes other than the quasi-TEM mode propagating at the outside of the cable screen), which would be relevant only at frequencies typically larger than 1 GHz for a cable "near" a ground plane. The present experimental results and the theoretical results of § VIII of [8], show that at least type 3 and type 5 couplings play a significant role above 100 kHz for typical cables.

2. The theory that describes the five modes of coupling is not directly related to the theory of the internal quasi-TEM modes of propagation on the multiconductor transmission line inside the cable screen. In fact, the theory shows that different values than the one obtained for using only from type 1 and type 2 couplings must be used for the internal distributed "equivalent" voltage and current sources due to the external fields.

3. Taking into account types of coupling other than type 1 and type 2 is not an unnecessary refinement. The calculations presented in § III for the case of transverse incidence, and the experiments of § IV and § V show simple situations when type 3 or type 5 coupling dominate the cable response.

Acknowlegements

We want to mention the contribution of Mr. Daniel Negret of CEG (Gramat) who led the GTEM measurements, and of Mr. Daniel Givord of CTME (Arcueil) for the design of the cable samples. This work was supported by CTME.

References

[1] B. Demoulin, S. El Assad, P. Degauque, "Analysis of a two-wire shielded line in a disturbing environment", *Proceedings of the 7th International Zürich Symposium on EMC*, 3-5 March, 1987, pp. 181-185.

[2] P. Degauque, J. Hamelin, *Compatibilité électromagnétique*, Dunod, 1990.

[3] F. Broydé, E. Clavelier, "Comparison of Coupling Mechanisms on Multiconductor Cables", *IEEE Transactions on EMC*, Vol. 35, No. 4, pp. 409-416, November 1993.

[4] F. Broydé, E. Clavelier, D Givord, P. Vallet, "Discussion of the relevance of Transfer Admittance and Some Through Elastance Measurement Results", *IEEE Transactions on EMC*, Vol. 35, No. 4, pp. 417-422, November 1993.

[5] Patent application # 93 10903 (France), "Dispositif pour la caractérisation des imperfections de câble avec écran par application d'un champ magnétique variable transverse à l'axe du câble", inventors : F. Broydé, E. Clavelier.

[6] Patent application # 93 13492 (France), "Dispositif pour la caractérisation des imperfections de câble avec écran par application d'un champ magnétique variable parallèle à l'axe du câble", inventors : F. Broydé, E. Clavelier.

[7] F. Broydé, E. Clavelier, "Complément à la théorie du couplage champ à câble : définition des cinq modes de couplage et mesure des impédances de transfert axiales et paralleles", *Proceedings of the 7ième Colloque International sur la CEM "RCEM 94"*, Toulouse 2-4 mars 1994, pp 463-470.

[8] F. Broydé, E. Clavelier, "Measurement of the Parallel and Axial Transfer Impedances : Theory, Practical Methods and Results", *Proceedings of the 1994 EUROEM conference*, Bordeaux, to be published.

[9] F. Broydé, E. Clavelier, "Parallel and Axial Transfer Impedances : Theoretical Summary and Local Measurement Methods", *Proceedings of the 11th International Zürich Symposium on EMC*, Zürich, March 7-9, 1995, to be published.